POLITECNICO DI TORINO
Repository ISTITUZIONALE

Conceptual structural design and analysis of a 20 T hybrid cos-theta dipole for future particle colliders

Original
Conceptual structural design and analysis of a 20 T hybrid cos-theta dipole for future particle colliders / D'Addazio, M., Ferracin, P., Marinozzi, V., Ravaioli, E., Vallone, G., Savoldi, L.. - In: IEEE TRANSACTIONS ON APPLIED SUPERCONDUCTIVITY. - ISSN 1558-2515. - ELETTRONICO. - 35:(2025). [10.1109/TASC.2024.3513274]

Availability:
This version is available at: 11583/3003468 since: 2026-04-08T08:59:38Z

Publisher:
Institute of Electrical and Electronics Engineers Inc.

Published
DOI:10.1109/TASC.2024.3513274

Terms of use:

This article is made available under terms and conditions as specified in the corresponding bibliographic description in the repository

Publisher copyright
IEEE postprint/Author's Accepted Manuscript

©2025 IEEE. Personal use of this material is permitted. Permission from IEEE must be obtained for all other uses, in any current or future media, including reprinting/republishing this material for advertising or promotional purposes, creating new collecting works, for resale or lists, or reuse of any copyrighted component of this work in other works.

(Article begins on next page)

03 November 2026

This article has been accepted for publication in IEEE Transactions on Applied Superconductivity. This is the author's version which has not been fully edited and content may change prior to final publication. Citation information: DOI 10.1109/TASC.2024.3513274

Conceptual Structural Design and Analysis of a 20 T Hybrid Cosθ Dipole for Future Particle Colliders

Marika D'Addazio, Paolo Ferracin, *Senior Member, IEEE*, Vittorio Marinozzi, Emmanuele Ravaioli, Giorgio Vallone, Laura Savoldi, *Member, IEEE*

***Abstract*—To reach high collision energy for future high-energy particle colliders, like the Future Circular Collider (FCC) or the Muon Collider, it is required to achieve high field strength of the bending dipoles. Currently, the practical limit for Nb_3Sn technology is around 16 T and, in order to further increase the magnetic field, the superconducting magnet community is considering High Temperature Superconductors (HTS), in particular Bi-2212 and REBCO conductors. However, their relevant higher cost has led the community to consider a hybrid approach where HTS materials are used in the high field region of the coils with so-called "insert coils", and Low Temperature Superconductors are involved in the lower field part (<16 T) with so-called "outsert coils". This paper describes the conceptual mechanical design of a 20 T hybrid cosθ dipole configuration. The high stress levels that the structure is facing due to the high magnetic field are discussed. Moreover, it presents the results of the optimization analysis of the shell-based support structure based on the key-and-bladder technology that provides the azimuthal pre-stress during room temperature assembly and cooldown to cryogenic temperatures. The aim of this work is to present a feasible design that satisfies the stress requirements.**

***Index Terms*—Superconducting magnets, dipole, hybrid magnets, HTS, Nb3Sn, mechanical analysis.**

I. Introduction

THE US Magnet Development Program (MPD) is leading a design study group for conducting a research on accelerator magnets targeting a bore field of 20 T for the next generation of particle colliders [1], [2]. For a magnet with this level of field, the first proposal was explored in 2005 with a 24 T dipole magnet with the attempt of triple the nominal field of 8.3 T of the LHC dipoles [3]. In 2011, different design studies were focused on dipoles with a 20 T bore field to start introducing the idea of a 16.5 TeV beam energy accelerator in the LHC tunnel [4]–[6]. A similar operational field was also considered for the Super proton-proton Collider (SppC) in China [7], [8] and for the European Future Circular Collider (FCC) [9].

Automatically generated dates of receipt and acceptance will be placed here.

This work is part of the project PNRR-NGEU which has received funding from the MUR – DM 118/2023.

This work is supported by the Office of High Energy and Nuclear Physics, U. S. Department of Energy, under contract No. DE-AC02-05CH11231.

M. D'Addazio is with Politecnico di Torino, 10129 Torino (TO), Italy and Lawrence Berkeley National Laboratory, Berkeley, CA 94720 USA (e-mail: marika.daddazio@polito.it).

P. Ferracin and G. Vallone are with Lawrence Berkeley National Laboratory, Berkeley, CA 94720 USA.

E. Ravaioli is with the European Organization for Nuclear Research (CERN), 1211 Geneva, Switzerland.

M. Marinozzi is with Fermi National Accelerator Laboratory, Batavia, IL 60510 USA.

L. Savoldi is with Politecnico di Torino, 10129 Torino (TO), Italy and Istituto Nazionale di Fisica Nucleare, sez. Genova, Italy.

Colour versions of one or more of the figures in this paper are available online at xx.

Digital Object Identifier: xx.

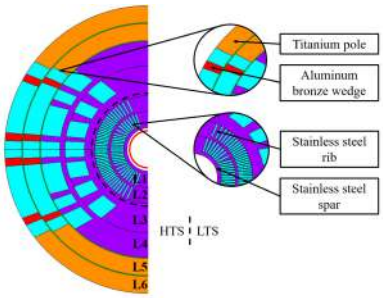


Fig. 1. 2D cross-section of the dipole. The black dashed line separates the HTS from LTS parts. The red line represents the magnet aperture. On the right, the magnified portions of the dipole show the mandrel components (spar and rib) and the parts of the traditional cosθ design (pole and wedge).

TABLE I
DESIGN CRITERIA OF THE MAGNET [2]

Bore magnetic field (T)	20.0
Bore diameter (mm)	50
Operating temperature (K)	1.9
Margin, $(I_{ss}\text{-}I_{op})/I_{op}$ (-)	15%
Geometrical harmonics (unit) at $R_{ref} = 17$ mm	<3
Max stress Nb_3Sn at 1.9 K (MPa)	180
Max stress Bi-2212 at 1.9 K (MPa)	120

The practical limit of 16 T for the Nb_3Sn accelerator magnets does not allow the only use of Low Temperature Superconductors (LTS) for reaching the target field of 20 T. Therefore, a possible option consists in the introduction of a hybrid concept where the High Temperature Superconductors (HTS) are employed in the high field region of the coils and the LTS conductor in the lower field region. The hybrid approach has also the advantage of reducing the overall cost of the dipole considering the current high cost of HTS.

This paper presents the design of a realistic structural layout for a 20 T hybrid cosθ dipole magnet, addressing the challenges of managing high stresses at such a high field level. The analysis of the 2D magnet cross-section is a crucial preliminary step for establishing the feasibility of such a challenging dipole magnet. The study focuses on the optimization of the 2D magnet cross-section with an infinitely rigid structure, followed by the introduction of an external iron structure to simulate more realistic conditions. A significant aspect of this study is evaluating the azimuthal pre-stress applied using key and bladder technology, which helps the

© 2024 IEEE. Personal use is permitted, but republication/redistribution requires IEEE permission. See https://www.ieee.org/publications/rights/index.html for more information.

This article has been accepted for publication in IEEE Transactions on Applied Superconductivity. This is the author's version which has not been fully edited and content may change prior to final publication. Citation information: DOI 10.1109/TASC.2024.3513274

TABLE II
MAIN CONDUCTOR PARAMETERS

Parameter	L1-L2	L3-L4	L5-L6
Superconductor/Stabilizer	Bi-2212/Ag	Nb_3Sn /Cu	Nb_3Sn /Cu
Number of strands (-)	32	50	50
Strand diameter (-)	0.90	0.80	0.70
Ag/noAg or Cu/noCu (-)	4.00	0.90	2.00
Cable width (mm)	14.87	22.16	19.39
Cable average thick. (mm)	1.70	1.52	1.33
Insulation thickness (mm)	0.15	0.15	0.15
Operating current (A)	11593	11593	11593
Current density J_e at I_{op} (A/mm^2)	569	461	602
Peak field at I_{op} (T)	20.46	16.12	12.75

magnet structure withstand the Lorentz forces. The novelty of this work lies in demonstrating a viable structural design that meets the stress requirements and identifying the possible critical points, setting the stage for future magnets in high-energy particle colliders.

II. CROSS-SECTION ASSUMPTIONS

A. Design criteria

The dipole magnet under study is designed to reach a magnetic field of 20 T in a 50 mm clear bore represented by the red circle in Fig. 1. The main design criteria of the magnet are summarized in Table I. The maximum allowed geometrical harmonics are 3 units at the reference radius of 17 mm. The load-line margin, defined as $(I_{ss}\text{-}I_{op})/I_{op}$ with I_{ss} the short sample current and I_{op} the operational one, is required to be 15%.

The conductors selected for the design study are Bi-2212 (HTS) and Nb_3Sn (LTS) designed as Rutherford cables made of multi-filamentary strands. The black dashed line in Fig. 1 indicates the separation between the HTS and LTS conductors. To avoid conductor degradation, the limit on the Von Mises equivalent stress is imposed to 180 MPa for the Nb_3Sn and 120 MPa for the Bi-2212.

B. 2D cross-section description

The optimization of the 2D magnet cross-section is performed assuming an infinitely rigid structure around the coils without considering pre-stress at room temperature. Numerous design were studied to find a solution that satisfy the selected requirements across the magnetic, the quench protection [10] and the mechanical analysis.

As described in detail in [11], the introduction of structural elements to intercept the electromagnetic forces in layers 1-4 was needed to reduce the stresses suffered by the conductors. In the innermost two layers, every conductor is separated from the previous and the following one by a structural component called rib. The mandrel of the magnet, as shown in Fig. 1, is composed by the so-called spar and ribs. This configuration can be realized with a CCT (Canted Cos-Theta) [12]–[14] or an SMCT (Stress Managed Cos-Theta) [15]–[17] layout, however the proposed 2D design is more representative of the SMCT one. The layers 3 and 4 are designed as a SMCT and the last two layers (layer 5-6) are standard Cos-Theta configuration made of titanium winding poles and aluminum bronze wedges.

Moreover, considering only the Nb_3Sn coils, the dimension of the conductors is gradually reduced while moving further from the magnet bore (grading). The cable width ranges from 19.39 mm in layers 5-6 to 22.16 mm in layers 3-4. Using smaller cables where the magnetic field is lower is useful to reduce the overall size of the dipole and to be more efficient by taking advantage of the lower field working region of the LTS conductors. The other conductor parameters are summarized in Table II.

III. MECHANICAL DESIGN

A. Modeling assumptions

The magnetic and mechanical analysis are performed using ANSYS APDL. The Lorentz forces are evaluated with the magnetic analysis and directly transferred to the mechanical simulations. The elements PLANE53 and PLANE183 are respectively used for the magnetic and mechanical simulations considering the plane stress condition.

In the design study, the LTS and HTS coils are simulated as a homogenized material (block model). The Nb_3Sn elasto-plastic properties [18] are retained for both LTS and HTS conductors. According to [19], the elastic properties of Bi-2212 are similar to the Nb_3Sn ones, therefore it could be assumed that the same similarity persists in the elasto-plastic regime. The Nb_3Sn properties are extracted from the sub-model of a cable stack that well matched the measurements performed on MQXF magnets, a quadrupole developed for the High Luminosity LHC project [20]. The mechanical properties of the structural components are provided in [18].

The interfaces between the conductors and the mandrels in layers 1-4 are simulated allowing sliding and separation, assuming a friction coefficient of 0.2. The coils of layers 5 and 6 have coupled nodes with the respective wedges and the separation with the poles is allowed.

B. Preliminary rigid structure

The analysis performed with the infinitely rigid structure provides in general non-conservative results in terms of conductor stresses. Indeed, the deformability of the structure is expected to increase the stresses. Therefore, a more realistic boundary condition was introduced to verify the imposed limit on the Von Mises equivalent stress for the conductors and to provide a guide for the design of a realistic structure. The analysis was performed by introducing an external structure simplified with a closed cylindrical ring of iron around the coils shown on the bottom of Fig. 2. In these simulations, only the Lorentz forces are applied.

The analysis was performed by varying the thickness of the external iron structure while maintaining the operational bore field equal to 20 T. For a given 2D cross-section designed to fulfill the load-line margin of 15%, it is possible to evaluate the influence of the variation of the iron thickness on the load-line margin itself as shown in Fig. 2. The load-line margin of the HTS layers increases with increasing the thickness of the external ring of iron, while for layers 3-4 the results are almost stable after considering a thickness of 100 mm.

© 2024 IEEE. Personal use is permitted, but republication/redistribution requires IEEE permission. See https://www.ieee.org/publications/rights/index.html for more information.

This article has been accepted for publication in IEEE Transactions on Applied Superconductivity. This is the author's version which has not been fully edited and content may change prior to final publication. Citation information: DOI 10.1109/TASC.2024.3513274

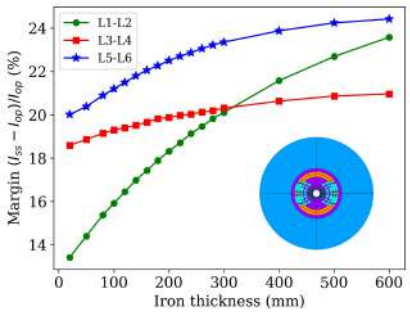
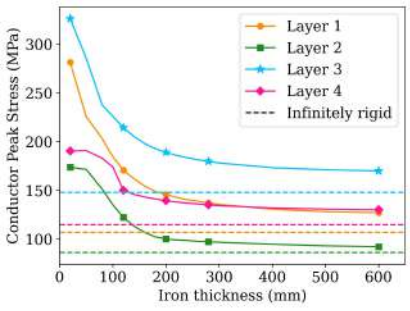
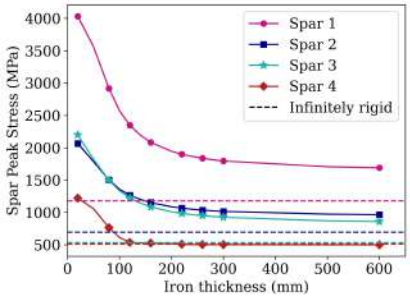


Fig. 2. Variation of the load-line margin (I_{ss}-I_{op})/I_{op} as a function of the iron thickness for all the magnet layers. The HTS layers are identified as L1-L2 and the LTS layers are identified as L3-L4 and L5-L6.



(a)



(b)

Fig. 3. Von Mises equivalent stress in the conductors (a) and in the mandrels (b) of the stress managed layers 1-4 as a function of the iron thickness variation. The dashed lines represent the results evaluated with an infinitely rigid structure.

To evaluate the effect of the external iron thickness, the Von Mises equivalent stresses were verified. The peak stresses evaluated in the conductors and at the inner radius of the spars of layers 1-4 are respectively shown in Fig. 3(a) and Fig. 3(b). The Von Mises stresses are only shown for the layers where the stress management design was introduced. The dashed lines represent the equivalent stress retrieved with the infinitely rigid structure. The results confirm that this ideal condition provides non-conservative results when compared to the ones actually achieved with a more realistic boundary condition. In Fig. 3(a), this is visible in layers 1 and 3: the results with the external ring of iron at 300 mm thickness are respectively equal to 136 MPa and 178 MPa while the peak stresses with the infinitely rigid structure are equal to 107 MPa and 148 MPa. In Fig. 3(b), the spar results of layers 2 and 3 are similar and in general

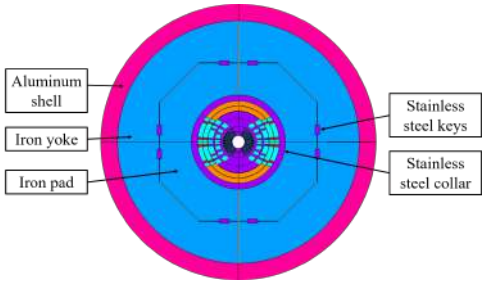


Fig. 4. The 2D cross-section of the structure for the hybrid cosθ dipole design.

lower than the one of layer 1. After 100 mm, the stresses of the layer 4 spar are comparable with the infinitely rigid structure result. At 300 mm thickness of the external structure, the peak stresses of the spars 1 and 2 are respectively around 1795 MPa and 1015 MPa. After an iron thickness of around 200 mm, the variation of the peak stress in both the conductors and the spars starts to become negligible.

C. Real mechanical structure

The mechanical structure of the magnet is shown in Fig. 4. The structure is composed by the stainless steel collar surrounding the coils, the iron pad and yoke, and the aluminum shell.

Three sequential load steps were considered. In the first load step, the pre-stress at room temperature is provided by the bladder and key technology [21]. The bladders and the keys are inserted between the pad and the iron yoke. The keys are made of stainless steel and to apply the pre-stress at room temperature, an horizontal interference has been added. In the current cross-section the bladder slot has not been included yet.

In the second load step, the cooldown to the cryogenic temperature of 1.9 K is considered. The aluminum shell that is surrounding the iron yoke provides a further increase of the pre-stress during the cooldown [22].

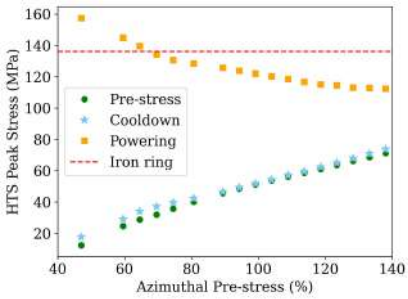
In the third final load step, the Lorentz forces at a bore field of 20 T are applied.

The structure components are dimensioned to comply with the material limits and the pre-stress requirements. Initially, the overall thickness including both the iron pad and the yoke was equal to 200 mm, the minimum overall thickness needed to guarantee low stresses, as shown in Fig. 3. At 200 mm, the conductor peak stresses were below the limit with a sufficient amount of azimuthal pre-stress but the mechanical structure was not able to handle the high stresses involved. After simulating different designs, the solution with a total thickness for pad and yoke of 300 mm was the one that satisfied both the conductors and the structure requirements. The overall diameter of the current 2D magnet cross-section is equal to 1.12 m.

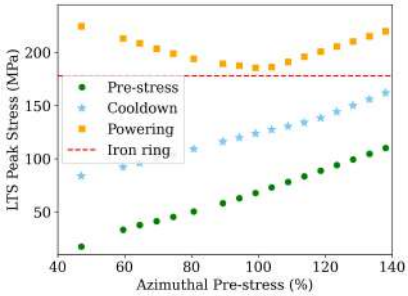
To define the optimum azimuthal pre-compression value to apply at room temperature, a parametric analysis was performed and the results are shown in Fig. 5. The dashed lines in red represent the Von Mises equivalent stress calculated by

© 2024 IEEE. Personal use is permitted, but republication/redistribution requires IEEE permission. See https://www.ieee.org/publications/rights/index.html for more information.

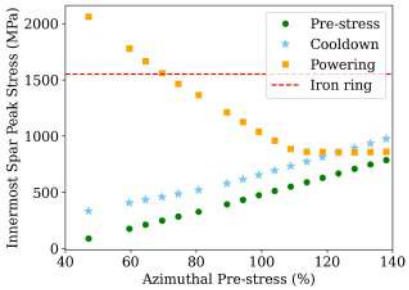
This article has been accepted for publication in IEEE Transactions on Applied Superconductivity. This is the author's version which has not been fully edited and content may change prior to final publication. Citation information: DOI 10.1109/TASC.2024.3513274



(a)



(b)

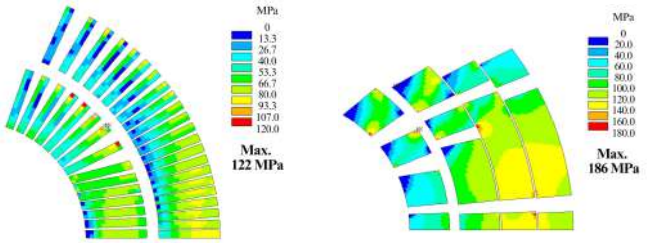


(c)

Fig. 5. Von Mises equivalent stress after each load step in the HTS (a) and LTS (b) conductors and in the inner radius of the spar of layer 1 (c) as a function of the azimuthal pre-stress in percentage. The dashed line represents the results evaluated introducing a more realistic boundary condition, the cylindrical ring of iron.

introducing the ideal iron structure (shown in Fig. 2). The stresses with the real mechanical structure are evaluated in all the phases (pre-stress at room temperature, cooldown at cryogenic temperature and introduction of the Lorentz forces), considering an overall iron thickness of 300 mm and adjusting only the applied pre-stress. The optimum equivalent stress value can be reached by assuming an azimuthal pre-stress in the range of 95-100% of the electromagnetic forces. The plots in Fig. 5 show that is possible to achieve a stress distribution in the conductors and in the innermost spar that is even better than the one evaluated with the external iron structure described in Section III-B.

In Fig. 5(c), the equivalent peak stress is evaluated at the inner radius location of the first layer spar, which experiences higher stresses as shown in Fig. 3(b). Considering an azimuthal pre-stress of 100% of the electromagnetic forces, the stress is around 1040 MPa at energization. This confirms that applying an azimuthal pre-stress improves the stresses in the spar. Regarding the ribs of layers 1-4, the peak stress is unreliable due to fictitious stresses localized at the corners; the development of a sub-model is needed to determine the real maximum stress value. This evaluation would enable to identify the most suitable material for the mandrels to withstand these loads. A possible solution is using a high strength stainless steel (as an example, Nitronic 40) or Inconel.



(a) (b)

Fig. 6. Von Mises equivalent stress (MPa) in the HTS (a) and LTS (b) conductors after energization. The maximum stress values are also reported.

In Fig. 6 are shown the equivalent stress contour plots for both HTS and LTS after energization. Regarding the HTS conductors in Fig. 6(a), the recorded peak stress is 122 MPa located in a small corner of layer 1; for the LTS conductors in Fig. 6(b), the peak stress is 186 MPa and the maximum is located in the third block of layer 3.

IV. Conclusion

In this paper, the conceptual mechanical design of a 20 T hybrid cosθ dipole magnet for future particle accelerators is presented. The magnet is composed by HTS conductors in the higher field region of the coils and LTS conductors in the lower field region. This hybrid approach is a promising option to reach high magnetic field.

The optimization of the 2D dipole cross-section assuming an infinitely rigid structure around the coils provides a solution that meets the design criteria requirements. However, the introduction of a more realistic boundary condition results in an overall increase of the stresses in the conductors and in the mandrels of layers 1-4. Applying an azimuthal pre-stress equal to 95-100% of the electromagnetic forces is required to reduce the stresses in the conductors and in the spars. The dimensions of the real structure components are defined to preserve the overall integrity and to satisfy the pre-stress requirements. The current overall diameter of the 2D magnet cross-section is equal to 1.12 m. The peak stresses in the HTS and LTS conductors are respectively equal to 122 MPa and 186 MPa. The stresses in the ribs are still under investigation.

Further optimization of the mechanical structure is planned to study the effect on the stresses of all the available parameters such as the key position and the shape of the iron components. Moreover, the 3D analysis is planned in the future to investigate the forces and evaluate the stress and the strain in the coil ends which were not accounted for in the 2D analysis results.

© 2024 IEEE. Personal use is permitted, but republication/redistribution requires IEEE permission. See https://www.ieee.org/publications/rights/index.html for more information.

This article has been accepted for publication in IEEE Transactions on Applied Superconductivity. This is the author's version which has not been fully edited and content may change prior to final publication. Citation information: DOI 10.1109/TASC.2024.3513274

REFERENCES

[1] P. Ferracin *et al.*, "Towards 20 T Hybrid Accelerator Dipole Magnets," in *IEEE Transactions on Applied Superconductivity*, vol. 32, no. 6, pp. 1-6, Sept. 2022, Art no. 4000906, doi: 10.1109/TASC.2022.3152715.

[2] P. Ferracin *et al.*, "Conceptual Design of 20 T Hybrid Accelerator Dipole Magnets," in *IEEE Transactions on Applied Superconductivity*, vol. 33, no. 5, pp. 1-7, Aug. 2023, Art no. 4002007, doi: 10.1109/TASC.2023.3250382.

[3] P. McIntyre and A. Sattarov, "On the Feasibility of a Tripler Upgrade for the LHC", PAC (2005) 634.

[4] L. Rossi and E. Todesco, "Conceptual design of 20 T dipoles for high-energy LHC," CERN, Geneva, Switzerland, CERN Yellow Rep. 2011-3, pp. 13–19, 2011.

[5] E. Todesco, *et al.*, "Dipoles for High-Energy LHC", *IEEE Transactions on Applied Superconductivity*, vol. 24, no. 3, June 2014, Art. no. 4004306.

[6] R. Gupta, *et al.*, "Hybrid High-Field Cosine-Theta Accelerator Magnet R&D With Second-Generation HTS", *IEEE Transactions on Applied Superconductivity*, vol. 25, no. 3, June 2015, Art. no. 4003704.

[7] G. Sabbi,*et al.*, https://indico.ihep.ac.cn/event/4900.

[8] Qingjin Xu, *et al.*, "20-T Dipole Magnet with Common-Coil Configuration: Main Characteristics and Challenges", *IEEE Transactions on Applied Superconductivity*, vol. 26, no. 4, June 2016, Art. no. 4000404.

[9] J. van Nugteren, *et al.*, "Toward REBCO 20 T+ Dipoles for Accelerators", *IEEE Transactions on Applied Superconductivity*, vol. 28, no. 4, June 2018, Art. no. 4008509.

[10] E. Ravaioli, *et al.*, "Quench Protection Analysis of 20 T Hybrid Accelerator Dipole Magnets", submitted to *IEEE Transactions on Applied Superconductivity*, September 2024.

[11] V. Marinozzi, *et al.*, "Conceptual design of a 20 T hybrid cos-theta dipole superconducting magnet for future High-Energy particle accelerators.", (2022).

[12] S. Caspi, *et al.*, "Design of a Canted-Cosine-Theta Superconducting Dipole Magnet for Future Colliders," in *IEEE Transactions on Applied Superconductivity*, vol. 27, no. 4, pp. 1-5, June 2017, Art no. 4001505, doi: 10.1109/TASC.2016.2638458.

[13] B. Auchmann, *et al.*, "Electromechanical Design of a 16-T CCT Twin-Aperture Dipole for FCC," in *IEEE Transactions on Applied Superconductivity*, vol. 28, no. 3, pp. 1-5, April 2018, Art no. 4000705, doi: 10.1109/TASC.2017.2772898.

[14] L. Brouwer, *et al.*, "Design of CCT6: A Large Aperture, Nb_3Sn Dipole Magnet for HTS Insert Testing," in *IEEE Transactions on Applied Superconductivity*, vol. 32, no. 6, pp. 1-5, Sept. 2022, Art no. 4001805, doi: 10.1109/TASC.2022.3151723.

[15] A. Zlobin, *et al.*, "Large-Aperture High-Field Nb_3Sn Dipole Magnets", in *Proc. Int. Part. Accel. Conf.*, 2018, paper WEPML026.

[16] I. Novitski,*et al.*, "Development of a 120-mm Aperture Nb_3Sn Dipole Coil With Stress Management," in *IEEE Transactions on Applied Superconductivity*, vol. 32, no. 6, pp. 1-5, Sept. 2022, Art no. 4006005, doi: 10.1109/TASC.2022.3163062.

[17] A. Patoux, *et al.*, "Test of New Accelerator Superconducting Dipoles Suitable for High Precision Field," in *IEEE Transactions on Nuclear Science*, vol. 30, no. 4, pp. 3681-3683, Aug. 1983, doi: 10.1109/TNS.1983.4336765.

[18] G. Vallone, *et al.*, "A Review of the Mechanical Properties of Materials Used in Nb_3Sn Magnets for Particle Accelerators," in *IEEE Transactions on Applied Superconductivity*, vol. 33, no. 5, pp. 1-6, Aug. 2023, Art no. 4002806, doi: 10.1109/TASC.2023.3248544.

[19] L. Pei, *et al.*, "Thermal-mechanical properties of epoxy-impregnated Bi-2212/Ag composite," in *IEEE Transactions on Applied Superconductivity*, vol. 25, no. 3, pp. 1-4, June 2015, Art no. 8400904, doi: 10.1109/TASC.2014.2376178.

[20] G. Vallone, *et al.*, "A methodology to compute the critical current limit in Nb_3Sn magnets", in *Supercond. Sci. Technol.*, 2021, doi: 10.1088/1361-6668/abc56b.

[21] S. Caspi and P. Ferracin, "Limits of Nb_3Sn Accelerator Magnets," in *Proc. Part. Accel. Conf.*, 2005, pp. 107-111, doi: 10.1109/PAC.2005.1590372.

[22] S. Caspi, *et al.*, "The use of pressurized bladders for stress control of superconducting magnets," in *IEEE Transactions on Applied Superconductivity*, vol. 11, no. 1, pp. 2272-2275, March 2001, doi: 10.1109/77.920313.

© 2024 IEEE. Personal use is permitted, but republication/redistribution requires IEEE permission. See https://www.ieee.org/publications/rights/index.html for more information.